HOKKAIDO UNIVERSITY

Title	Novel polychrome staining distinguishing osteochondral tissue and bone cells in decalcified paraffin sections
Author(s)	Nakamura, Teppei; Sumi, Kanako; Tsuji, Erika; Hosotani, Marina; Namba, Takashi; Ichii, Osamu; Irie, Takao; Nagasaki, Ken-ichi; Kon, Yasuhiro; Mishima, Takashi; Yoshiyasu, Tomoji
Citation	Cell and tissue research, 385, 727 https://doi.org/10.1007/s00441-021-03516-6
Issue Date	2021-08-19
Doc URL	http://hdl.handle.net/2115/86586
Rights	This is a post-peer-review, pre-copyedit version of an article published in Cell and tissue research. The final authenticated version is available online at: http://doi.org/10.1007/s00441-021-03516-6
Type	article (author version)
File Information	Cell and tissue research_s00441-021-03516-6.pdf

1 **Title: Novel Polychrome Staining Distinguishing Osteochondral Tissue and Bone Cells in**

2 **Decalcified Paraffin Sections**

3 **Authors**: Teppei Nakamura[1,2], Kanako Sumi[1], Erika Tsuji[1], Marina Hosotani[3], Takashi Namba[2], Osamu

4 Ichii[2, 4], Takao Irie[5, 6], Ken-ichi Nagasaki[7], Yasuhiro Kon[2], Takashi Mishima[1], Tomoji Yoshiyasu[1]

5 **Affiliation**s:

6 [1] Department of Biological Safety Research, Chitose Laboratory, Japan Food Research Laboratories,

7 Chitose, Hokkaido 066-0052, Japan

8 [2] Laboratory of Anatomy, Department of Basic Veterinary Sciences, Division of Veterinary Medicine,

9 Faculty of Veterinary Medicine, Hokkaido University, Sapporo, Hokkaido 060-0818, Japan

10 [3] Laboratory of Veterinary Anatomy, Department of Veterinary Medicine, School of Veterinary Medicine,

11 Rakuno Gakuen University, Ebetsu, Hokkaido 069-8501, Japan

12 [4] Laboratory of Agrobiomedical Science, Faculty of Agriculture, Hokkaido University, Sapporo,

13 Hokkaido 060-0818, Japan

14 [5] Medical Zoology Group, Department of Infectious Diseases, Hokkaido Institute of Public Health,

15 Sapporo, Hokkaido 060-0818, Japan

16 [6] Laboratory of Veterinary Parasitology, Faculty of Agriculture, University of Miyazaki, Miyazaki, 889-

17 2192, Japan

18 [7] Department of Biological Safety Research, Tama Laboratory, Japan Food Research Laboratories, Tama,

19 Tokyo 206-0025, Japan

20 **Corresponding author**: Teppei Nakamura, D.V.M., Ph.D

21 Department of Biological Safety Research, Chitose Laboratory, Japan Food Research Laboratories,

22 Bunkyo 2-3, Chitose, Hokkaido 066-0052, Japan

23 Tel and Fax: +81-123-28-5113, E-mail: nakamurate@jfrl.or.jp

Abstract

The bone is a dynamic and metabolically active organ in which growth and resorption of the osteochondral matrix is orchestrated by osteoblasts and osteoclasts. For decalcified paraffin-embedded specimens, decalcifying agents alter the staining intensity, and excess decalcification interferes with bone staining. Robust bone staining methods independent of the decalcification conditions and animal species are lacking. In this study, we have developed a novel polychrome staining method, named JFRL staining, which stains the components of osteochondral tissue in different colors. With this staining we could visualize the hyaline cartilage as blue by alcian blue, osteoid as red by picrosirius red, and mineralized bone as green by picro-light green SF or picro-naphthol green B and easily distinguished osteoblasts, osteocytes, and osteoclasts. In mineralized bone, this staining revealed the obvious lamellar structures and woven bone. Notably, this staining was independent of the decalcification conditions and experimental animal species examined. To verify the usefulness of JFRL staining, we observed cotton rat tail which has shorter length and shows a false autotomy. The caudal vertebrae were normally developed via endochondral ossification without a fracture plane. At 6 months of age, the number of chondrocytes declined and the hypertrophic zone was absent at the epiphyseal plate, which might reflect the shorter tail. In conclusion, JFRL staining is the first method to simultaneously distinguish osteochondral matrix and bone cells in one section regardless of decalcifying conditions. This robust staining will provide new information for a wide number of biomedical fields, including bone development, physiology, and pathology.

Key Words: osteoid, mineralized bone, cartilage, bone cells, osteochondral staining

Introduction

Bone is a dynamic and metabolically active organ in which simultaneous growth and resorption of the bone matrix is orchestrated by osteoblasts and osteoclasts under hormonal regulation. The bone is formed via two pathways: intramembranous ossification and endochondral ossification (Gilbert 2000). During development, flat bones are formed by intramembranous ossification, where osteoblasts differentiate directly from mesenchymal stem cells to form the bone matrix. In contrast, long bones are formed by endochondral ossification, where chondrocytes differentiate from mesenchymal stem cells to produce cartilage, and the mineralized cartilage is replaced by the bone matrix (Gilbert 2000). After birth, both processes remain, and the latter is found at the epiphyseal plate of the long bones and temporarily during bone healing after fracture (Moreira et al. 2000; Bahney et al. 2019). The epiphyseal plate consists of reserve (resting), proliferative, and hypertrophic zones depending on the stages of chondrocyte differentiation (Roach et al. 2003). The bone matrix is composed of two elements—the osteoid bone and calcified bone. Osteoid, the newly formed unmineralized bone matrix composed of type I collagen, is produced by osteoblasts (Moreira et al. 2000). The osteoid becomes filled with calcium phosphate to form the mature form—calcified bone, and osteoblasts differentiate into mature form, osteocytes. The old or damaged calcified bone is removed by osteoclasts. Mineralized bone is morphologically visualized as two types. When the bone is formed rapidly during development and during fracture healing, it is not tightly packed and is called woven bone (Moreira et al. 2000). Woven bone is progressively replaced by mature lamellar bone (Moreira et al. 2000).

An imbalance between osteoblast-mediated bone formation and osteoclast-mediated resorption may lead to abnormal bone remodeling and bone disorders. Osteomalacia is exhibited by elevated osteoid formation due to delayed bone mineralization, whereas other disorders such as hypoparathyroidism increases mineralized bone due to excess mineralization (Kulak and Dempster 2010). Humans, companion

animals, and laboratory animals all develop bone metabolic diseases and diagnosis of these metabolic bone diseases requires a histomorphometric analysis. As mentioned above, bone homeostasis is tightly regulated by complex processes. It is important to simultaneously stain the osteochondral matrix and bone cells in bone development, physiology, and pathology using rapid, robust, and, and highly reproducible staining methods.

Several staining methods can be used to distinguish the different components of the bone matrix. For undecalcified specimens, Villanueva osteochrome bone stain, or Villanueva-Goldner staining are routinely used to distinguish between osteoid and calcified bone (Ueno 1985). Other bone staining techniques can also be applied to decalcified paraffin-embedded specimens. Pretreatment with cyanuric chloride followed by hematoxylin and eosin increases the staining intensity of the osteoid (Yoshiki 1973). Movat's pentachrome, Masson-Goldner's trichrome, or Ralis tetrachrome staining stains the osteoid and mineralized bone with different colors (Ralis and Watkins 1992; Rentsch et al. 2014). Before these staining procedures, the bone specimens are decalcified using inorganic acids, organic acids, or chelators such as hydrochloric acid, formic acid, or ethylene diamine tetra acetic acid (EDTA), respectively (Bogoevski et al. 2019). Among the different decalcification agents, treatment with inorganic acid yields rapid decalcification, but has a high potential for tissue damage and also interferes with bone staining (Ralis and Watkins 1992; Bogoevski et al. 2019). To the best of our knowledge, no suitable staining is available for bone matrix with over-decalcification.

In this study, we have developed a novel polychrome staining method that simultaneously detects osteochondral tissues regardless of the decalcification method, and named it—Join of the Five dyes Revealing coLlagenous tissue (JFRL) staining. This staining also visualizes bone cells, such as osteoblasts, osteocytes, and osteoclasts unless the sections are over-decalcified. To clarify the usefulness of the JFRL staining, we examined the time-course changes of the caudal vertebrae in the cotton rats, *Sigmodon*

92   *hispidus*. The cotton rat is a rodent, classified in the family Cricetidae and has been selected as a laboratory

93   animal model in the field of infectious research because it can faithfully mimic human infectious diseases

94   (Niewiesk and Prince 2002). The cotton rats have a relatively shorter tail and show false caudal autotomy

95   characterized by loss of the tail sheath with the caudal vertebrae remaining (Faith et al. 1997; Hosotani et

96   al. 2021). Although the fracture plane of the skin has been clarified (Hosotani et al. 2021), those of the

97   caudal vertebrae have not yet been examined in cotton rats.

98

99   **Materials and methods**

100   *Animals and specimen preparation*

101   Animal experiments were performed in accordance with the guidelines of the Chitose Laboratory,

102   Japan Food Research Laboratories (approval no. HK200703-01) and the Hokkaido Institute of Public

103   Health (approval no. K30-01). Male animals of the following species were used in this study:

104   C57BL/6NCrSlc mice at 3 months of age (Japan SLC, Shizuoka, Japan), HIS/Hiph cotton rats of various

105   ages (maintained at Hokkaido Institute of Public Health), JclBrlHan:WIST rats at 2 months of age (CLEA

106   Japan, Tokyo, Japan), and Kbl:JW rabbits at 6 to 12 months of age (Kitayama Labes, Nagano, Japan). The

107   animals were euthanized with an intravenous injection of sodium pentobarbital in rabbits or by cutting the

108   abdominal aorta under deep anesthesia with isoflurane in mice, cotton rats, and rats. After euthanasia, the

109   femurs, tibiae, and caudal vertebrae were harvested, fixed with 10% neutral buffered formalin overnight

110   to 7 days at room temperature. After removal of the soft tissue, the fixed bones were decalcified with 10%

111   EDTA (pH 7.4, Muto Pure Chemicals, Tokyo, Japan), Morse's solution (pH 2.5, 10% sodium citrate and

112   20% formic acid, Fujifilm Wako Pure Chemical, Osaka, Japan), or K-CX solution (pH 0.2, 1.35 N HCl

113   and chelator, Falma, Tokyo, Japan) (Noda et al. 2007). The endpoint of decalcification was identified

114   when the microtome blade was inserted smoothly. Over-decalcification was confirmed by the loss of

115 nuclear staining with hematoxylin. The decalcified tissues were embedded in paraffin and cut into 4-μm

116 sections unless otherwise specified. Details of the bone samples are presented in Table 1.

117

118 *Reagents*

119   Weigert's iron hematoxylin, 1% Sirius red solution, saturated picric acid, 1% Alcian blue solution

120 (pH 2.5), 0.4% aniline blue solution, 0.75% orange G solution, and solution of 2.5% phosphotungstic acid

121 and 2.5% phosphomolybdic acid were purchased from Muto Pure Chemicals. Light green SF (Thermo

122 Fisher Scientific, MA, USA), fast green FCF (Nacalai Tesque, Tokyo, Japan), and naphthol green B

123 (Fujifilm Wako Pure Chemical) were also used. Picrosirius red (0.04%) was prepared by diluting 1%

124 Sirius red solution with saturated picric acid. The dilutions of 0.5% picro-light green, and 0.05% picro-

125 fast green, and 1% picro-naphthol green were prepared by diluting 2% solution of each dye with saturated

126 picric acid.

127

128 *Picrosirius red for osteoid staining*

129   For osteoid staining, deparaffinized sections were stained with 0.1% picrosirius red solution for 1 h

130 at room temperature and washed with 1% acetic acid. For alcian blue/picrosirius red staining,

131 deparaffinized sections were immersed in 3% acetic acid, stained with 1% alcian blue solution (pH 2.5)

132 for 30 min at room temperature, and rinsed with 3% acetic acid. The sections were then stained with 0.1%

133 or 0.04% picrosirius red for 5 min at room temperature and washed with 1% acetic acid. The sections

134 were dehydrated, cleared, and mounted with a coverslip using an acrylic resin (EUKITT®, ORSAtec,

135 Bobingen, Germany). The sections were observed using a BZ-X800 microscope (Keyence, Osaka, Japan)

136 with attached polarized filters.

137

138 *Selection of dyes for the mineralized bone*

139   To examine suitable dyes for mineralized bone, we modified the Masson's trichrome staining

140 protocol. Deparaffinized sections were stained with Weigert's iron hematoxylin for 10 min at room

141 temperature and washed in tap water. The sections were then immersed in 2.5% phosphotungstic acid and

142 2.5% phosphomolybdic acid for 1 min at room temperature, rinsed with 1% acetic acid, followed by

143 incubation in 0.75% orange G solution for 2 min at room temperature, and washed briefly in 1% acetic

144 acid. Mineralized bone was stained with aniline blue, fast green FCF, light green SF, or naphthol green B

145 solution in 1% acetic acid for 3 min at room temperature and rinsed with 1% acetic acid. The osteoid was

146 stained with 0.04% picrosirius red solution for 5 min at room temperature and rinsed with 1% acetic acid.

147 The sections were dehydrated, cleared, and mounted with a coverslip using an acrylic resin (EUKITT®,

148 ORSAtec). To examine the effect of picric acid as a mordant, the mineralized bone was also stained with

149 green dyes diluted with saturated picric acid, while 2.5% phosphotungstic acid and 2.5%

150 phosphomolybdic treatment was omitted.

151

152 *JFRL staining for osteochondral tissues and bone cells*

153   The procedure of JFRL staining developed in this study is as described below.

154   1. When staining for the cartilage, the sections were immersed in 3% acetic acid, then stained with

155   1% alcian blue solution (pH 2.5) for 20 min at room temperature, and rinsed with 3% acetic acid.

156   2. The sections were then stained with Weigert's iron haematoxylin for 10 min at room temperature

157   and washed in tap water. The differentiation step with hydrochloric acid can be omitted at this

158   stage, because the dye can be differentiated by the saturated picric acid present in the subsequent

159   steps.

160   3. The sections were then stained in 0.75% orange G solution for 2 min at room temperature and

161   washed briefly in 1% acetic acid.

162   4. This was followed by staining the sections with 0.05% picro-fast green FCF, 0.5% picro-light

163   green SF, or 1% picro-naphthol green for 3 min at room temperature and washed briefly in 1%

164   acetic acid for staining of the mineralized bone. When co-staining for the cartilage, fast green FCF

165   might be avoided due to its bluish color.

166   5. The sections were stained with 0.04% picrosirius red solution for 5–10 min at room temperature

167   and washed in 1% acetic acid.

168   6. The sections were finally dehydrated with graded alcohol, cleared with xylene, and mounted using

169   an acrylic resin (EUKITT®, ORSAtec). The slides were immersed in alcohol and xylene until the

170   removal of excess picric acid to achieve a good color balance.

171

172 **Results**

173 *Picrosirius red for osteoid staining*

174   First, we examined the staining methods which distinguish osteoid from mineralized bone, regardless

175 of animal species and decalcification methods. As reported previously (Junqueira et al. 1986), picrosirius

176 red caused red birefringence in the osteoid portion and a weaker green to orange birefringence in

177 mineralized bone under polarized light (Figs. 1a-d). The specificity of red birefringence in the osteoid was

178 independent of both the animal species and decalcifying agents. Notably, osteoid-specific birefringence

179 was maintained even in the over-decalcified specimen (Fig. 1d). When the same stained sections were

180 observed by light microscopy, 0.1% picrosirius red for 1 h stained the bone as red, but it was not specific

181 for the osteoid (Figs. 1a'-d'). In the over-decalcified specimen of the rat femur stained with 1% alcian

182 blue (pH 2.5), using a shorter staining time of 5 min with 0.1% picrosirius red increased the osteoid-

183 specific red color compared to those sections stained for 1 h (Figs. 1d' and e). However, the proliferating

184   zone of the epiphyseal plate was stained blue and red with a color overlap (Fig. 1e). In contrast, co-staining

185   of alcian blue and 0.04% picrosirius red for 5 min stained the osteoid as red and the cartilage as blue with

186   much less color overlap (Fig. 1e').

187

188   *Identification of suitable dyes for staining the mineralized bone*

189   We compared different dyes amongst the acidic dyes, with an aim to identify a suitable dye for the

190   staining of mineralized bone. The different dyes compared were aniline blue, fast green FCF, light green

191   SF, and naphthol green B. Rabbit femurs decalcified with inorganic acid were treated with 2.5%

192   phosphotungstic acid and 2.5% phosphomolybdic acid as a mordant. Aniline blue was more selective for

193   the osteoid rather than mineralized bone, and the osteoid was stained blue and red with a color overlap

194   (Figs. 2a-a''). In contrast, the other three dyes were more specific to mineralized bone, and the staining

195   intensity was concentration-dependent (Figs. 2b-d''). Fast green FCF tended to stain the mineralized bone

196   bluish in color than light green SF (Figs. 2b-b'' and c-c''), while naphthol green B stained them as

197   yellowish green with weaker staining intensity compared to light green SF (Figs. 2c-c'' and d-d''). In

198   addition, the combination of these green dyes and picrosirius red clearly revealed the lamellar structure of

199   green mineralized bone with repeated sequences of red lines (Figs. 2b-d''). The optimal concentration of

200   these dyes was 0.05% in fast green FCF, 0.2% to 0.5% in light green SF, and 0.5% to 1% in naphthol

201   green B.

202   Further, we also examined for a suitable specimen thickness and mordant for the combination of light

203   green SF and picrosirius red stains, and compared their staining specificity to picrosirius red staining under

204   polarized microscopy. At a specimen thickness of 2 or 4 µm, the mineralized bone was clearly

205   distinguished from the osteoid with a clear mineralization front in both the woven and lamellar bone (Figs.

206   3a and a'). Sections measuring more than 6 µm in thickness tended to increase the green intensity and

207 overlap with the red color in the osteoid, especially in the mineralization front (Figs. 3a'' and a'''). When

208 solution of 2.5% phosphotungstic acid and 2.5% phosphomolybdic acid was used as a mordant, 0.2% light

209 green SF tended to stain red blood cells which were already stained with Orange G as green (Fig. 3b).

210 Notably, 0.5% picro-light green SF kept erythrocytes orange and stained the mineralized bone more

211 greenish without decreasing staining intensity (Fig. 3b'). With either mordant, oval osteocyteswere found

212 in the lacunae of mineralized bone (Figs. 3b and b'). The specificity of osteoid by picrosirius red and

213 mineralized bone by light green SF was identical to picrosirius red staining under polarizing microscopy

214 (Figs. 3c-d').

215

216 *Visualization of osteochondral tissue and bone cells by JFRL staining*

217 The cartilage was not stained with either light green SF or picrosirius red stains (Fig. 3d). Therefore,

218 we stained the cartilage with 1% alcian blue (pH 2.5) and the osteoid with picrosirius red combined with

219 0.05% picro-fast green FCF, 0.5% picro-light green SF, and 1% picro-naphthol green B to observe

220 endochondral ossification. The rat femurs decalcified with organic acid or over-decalcified ones were used.

221 Because picro-fast green FCF colored the mineralized bone and hyaline cartilage as bluish green, the

222 mineralized bone was less indistinguishable from the hyaline cartilage (Figs. 4a and a'). Picro-light green

223 SF (Fig. 4b) and picro-naphthol green B (Fig. 4c) distinguished the hyaline cartilage, osteoid, and

224 mineralized bone by distinctly different colors (blue, red, and green, respectively) in the sections

225 decalcified with organic acid. The mineralized bone was stained weaker and more yellowish with picro-

226 naphthol green B compared with picro-light green SF staining (Figs. 4b and c). In the rat femur with over-

227 decalcification, although the proliferating zone of the epiphyseal plate was slightly co-stained with red

228 and blue, the hyaline cartilage, osteoid, and mineralized bone were all easily distinguishable (Figs. 4b'

229 and c'). In the sections decalcified with organic acid, osteoblasts and osteoclasts were easily identified.

230   The former was lined along the osteoid and had blackish cytoplasm, and the latter had large and greenish

231   cytoplasm and multiple nuclei (Figs. 4a-c). In the over-decalcified sections, the osteochondral tissue was

232   easily distinguished, although the nuclei were not stained, and osteoblasts and osteoclasts were less easily

233   identified (Figs. 4b' and c').

234   The overall staining characteristics of JFRL staining are summarized in Table 2. This novel

235   polychrome method stained the cartilage as blue by alcian blue, osteoid as red by Sirius red, and the

236   mineralized bone as green depending on the dye (Figs. 3 and 4). The nuclei were revealed as black, the

237   cytoplasm as various colors, and red blood cells as orange (Figs. 3 and 4). Osteoblasts and osteoclasts can

238   be distinguished by their cell shape; however, the nuclei were not stained in the over-decalcified sections

239   (Fig. 4). Osteocytes had oval shape and were localized in the lacunae of mineralized bone (Figs. 3b and

240   b').

241

242   *Time-course changes in the caudal vertebrae of cotton rats showing tail autotomy*

243   Using JFRL staining, we examined the time-course changes in the caudal vertebrae of cotton rats

244   (*Sigmodon hispidus*), which has a relatively shorter tail and shows false caudal autotomy (Faith et al. 1997;

245   Hosotani et al. 2021). On postnatal day 0, the caudal vertebrae were composed of hyaline cartilage, which

246   was observed as purple in their epiphyseal and blue in their diaphysis, and the periphery of the diaphysis

247   was surrounded by bone collar stained red and green (Figs. 5a and a'). On postnatal day 4, the hyaline

248   cartilage of the diaphysis was replaced by mineralized bone and bone marrow with cartilage absorption

249   by osteoclasts and osteoid secretion by osteoblasts (Figs. 5b and b'). The bone collar became thicker,

250   forming woven bone characterized by green and red matrix with irregular arrangement of osteoid and

251   osteocytes (Fig. 5b'). On postnatal day 7, the hyaline cartilage was almost replaced by the bone matrix

252   and bone marrow at the diaphysis (Fig. 5c), and primary trabeculae were slightly produced (Fig. 5c'). At

253   the juvenile age, the epiphyseal plate became obvious, and primary trabeculae extended toward the

254   diaphysis (Figs. 5d and d'). In contrast, the epiphyseal plate became thinner and the hypertrophic zone

255   was absent at the adult age (Figs. 5e and e'). A large region of the cartilage did not contain chondrocytes,

256   and the remaining cells were small (Fig. 5e'). Lamellar bone extending horizontally to the epiphyseal plate

257   and small bone formation was also found within the epiphyseal plate (Fig. 5e'). The fibrocartilage

258   consisting of the annulus fibrosus at the epiphyseal region was stained purple at postnatal day 0, which

259   became greenish with aging and was stained mainly green in juvenile age and thereafter (Figs. 5a''-e'').

260

261   **Discussion**

262   In this study, we developed a novel staining method called JFRL staining, which distinguishes the

263   osteochondral matrix and identifies bone cells. We also identified the staining dyes and concentrations

264   which were not affected by the decalcifying conditions and examined the staining protocol for robustness

265   and high reproducibility. The final procedure for JFRL staining is summarized in Supplemental Table 1.

266   This study demonstrated that the osteoid-specific birefringence by picrosirius red was independent

267   of decalcifying conditions, as observed even in over-decalcified sections under polarized microscopy.

268   Picrosirius red, which is a Sirius red solution diluted in saturated picric acid, visualizes the osteoid as red

269   birefringence under polarized microscopy (Junqueira et al. 1979, 1986). Sirius red specifically binds to

270   the [Gly-x-y] triple-helix structure in all collagen fibers and is used for the quantitative detection of all

271   types of collagen in histology and biochemistry (Kliment et al. 2011; Segnani et al. 2015). Osteoid and

272   mineralized bone contain 90% and 30% of type I collagen, respectively (Rosset and Bradshaw 2016). It

273   was previously shown that collagen fibrils do not degrade after decalcification (Fujita and Fujita 2002).

274   Therefore, the amount of collagen and preservation of their structures during decalcification might be the

275   reason for the distinguishing of the osteoid from the calcified bone by picrosirius red dye. In addition, a

276   lower concentration and shorter staining time of picrosirius red increased the staining specificity of the

277   osteoid under light microscopy. Consistent with this, picrosirius red is routinely used at a concentration

278   of 0.1% for polarized observation and at approximately 0.04% for light microscopy, similar to other

279   methods such as Sirius red/fast green and elastica van Gieson staining (Junqueira et al. 1986; Segnani et

280   al. 2015; Tomida et al. 2019). Taken together, these results highlight that picrosirius red is suitable for

281   osteoid staining under both polarized and light microscopy, regardless of decalcification conditions.

282   Since both calcified and osteoid bone contain type I collagen (Rosset and Bradshaw 2016), we chose

283   a dye compatible with calcified bone from the dyes—light green SF, fast green FCF, and naphthol green

284   B, commonly used for collagen staining. The results indeed showed that the calcified bone is stained green

285   similar to that in Masson-Goldner staining and Villanueva-Goldner staining, which uses light green SF

286   and naphthol green B, respectively (Junqueira et al. 1986; Rentsch et al. 2014; Nakata et al. 2016). By

287   using saturated picric acid as a mordant, mineralized bones were stained more yellowish compared to

288   staining seen when using 2.5% phosphotungstic acid and 2.5% phosphomolybdic acid as a mordant. In

289   addition, picric acid retained the orange stain in erythrocytes as stained by Orange G. Since fast green

290   FCF stained the mineralized bone as bluish green regardless of mordants, we argue that this dye might be

291   less suitable for co-staining the calcified bone and cartilage. Taken together, it can be concluded that picro-

292   light green SF is the most suitable dye for staining mineralized bone while simultaneously staining the

293   cartilage, osteoid, and calcified bone, all in one section, although we found that picro-naphthol green B

294   might also be useful.

295   Since the present study indicated that the novel staining we developed distinguished osteoid and

296   mineralized bone by the collagen content, we named it Join of the Five dyes Revealing coLlagenous tissue

297   (JFRL) staining. Notably, JFRL staining also distinguishes between lamellar bone and woven bone, and

298   among osteoblasts, osteocytes, and osteoclasts regardless of decalcification conditions and experimental

animal species examined. Recently, a trichrome staining was reported for musculoskeletal tissues using picrosirius red, fast green FCF, and alcian blue, which also differentiates osteoid and mineralized bone as red and green, respectively (Gaytan et al. 2020). However, unlike JFRL staining, both osteoid and the interterritorial matrix of hyaline cartilage were stained red, and the staining did not use iron hematoxylin and orange G for staining of the cellular components. Therefore, JFRL staining might be a more suitable method for osteochondral tissue, especially at the interface of osteocartilage.

To verify the usefulness of JFRL staining, we used the caudal vertebrae of cotton rats as a specimen for observing the histomorphology using JFRL staining. Cotton rats have unique phenotypes in their tail, that is, a shorter tail and false caudal autotomy characterized by loss of the tail sheath along the fracture plane with the caudal vertebrae remaining (Faith et al. 1997; Hosotani et al. 2021). Although the fracture plane of the skin has been clarified, those of the caudal vertebrae have not yet been examined in cotton rats. In addition, the histological characteristics of the shorter tail have not been identified until now. In the neonatal cotton rats, the caudal vertebrae were developed by endochondral ossification to form mineralized bone by osteoblasts and osteoclasts. At juvenile age of the cotton rats, the epiphyseal plates of caudal vertebrae had many chondrocytes and were replaced by spongy bone along longitudinal rows. In contrast, the South American rodent *Proechimys cuvieri* has a large area and loose structure of the epiphyseal plate, which functions as a fracture surface (Dubost and Gasc 1987). Therefore, it is hypothesized that cotton rats develop false caudal autotomy due to normal development of the caudal vertebrae without a fracture plane. In cotton rats at an adult age (6 months), which is much less than the lifespan of captive-bred cotton rats (usually 23 months) (Faith et al. 1997), the number of chondrocytes declined and the hypertrophic zone was absent at the epiphyseal plate. In addition, bones were formed parallel to the epiphyseal plate and within the epiphyseal plate. These changes are also observed in the long bones of rats that have reached their lifespan (Roach et al. 2003). This observation indicates that the

322 longitudinal extension of the caudal vertebra is lost at a younger age, which might reflect the shorter tail

323 in the cotton rats. As described above, JFRL staining unveiled histological characteristics of the bone

324 regarding caudal false autotomy and a shorter tail, and has been shown to be useful for examining bone

325 physiology.

326   In conclusion, JFRL staining, to the best of our knowledge, is the first method to simultaneously

327 distinguish cartilage, osteoid, and calcified bone, regardless of decalcification conditions and animal

328 species. This method also distinguishes between lamellar bone and woven bone, and among osteoblasts,

329 osteocytes, and osteoclasts. The novel JFRL staining will provide new information in a wide range of

330 biomedical fields, including bone development, physiology, and pathology. Although the current study

331 showed that JFRL staining is not dependent on the experimental animal species examined, further studies

332 using both normal bones and bone lesions in a wider range of animal species, including humans, are

333 required to further verify the robustness of this staining.

334

335 **Declarations**

336 **Conflicts of interests**

337   The authors have no conflicts of interest to declare that are relevant to the content of this article.

338

339 **Ethics approval**

340   Animal experiments were performed in accordance with the guidelines of the Chitose Laboratory,

341 Japan Food Research Laboratories (approval no. HK200703-01) and the Hokkaido Institute of Public

342 Health (approval no. K30-01).

343

344 **Authors' contributions**

345   Conception of the work: TN, OI, KN, YK, TM, TY

346   Design of the work: TN, OI, KN, YK, TM

347   Acquisition of data for the work: TN, KS, ET, MH, TN, TI,

348   Analysis of data for the work: TN, KS, ET, MH, TN,

349   Interpretation of data for the work: TN, KS, ET, TN, OI, YK, TM, TY

350   All authors have revised the manuscript, approved the final manuscript, and agreed to account for all

351   aspects of the work.

352

353   **References**

354   Bahney CS, Zondervan RL, Allison P et al. (2019) Cellular biology of fracture healing. J Orthop Res

355   37:35–50. doi: 10.1002/jor.24170

356   Bogoevski K, Woloszyk A, Blackwood K et al. (2019) Tissue morphology and antigenicity in mouse and

357   rat tibia: comparing 12 different decalcification conditions. J Histochem Cytochem 67:545–561.

358   doi:10.1369/0022155419850099

359   Faith RE, Montgomery CA, Durfee WJ et al. (1997) The cotton rat in biomedical research. Lab Anim Sci

360   47:337–345

361   Fujita H, Fujita T (2002) Textbook of histology Part 1, 4th edn. Igaku-Shoin, Tokyo, p 186 (in Japanese)

362   Gaytan F, Morales C, Reymundo C, Tena-Sempere M (2020) A novel RGB-trichrome staining method

363   for routine histological analysis of musculoskeletal tissues. Sci Rep 10:16659. doi: 10.1038/s41598-

364   020-74031-x

365   Gilbert SF (2000) Osteogenesis: the development of bones. In: Developmental biology, 6th edn.

366   https://www.ncbi.nlm.nih.gov/books/NBK10056/ Sinauer Associates, Sunderland (MA)

367   Hosotani M, Nakamura T, Ichii O et al. (2021) Unique histological features of the tail skin of cotton rat

368   (*Sigmodon hispidus*) related to caudal autotomy. Biol Open 10:bio058230. doi: 10.1242/bio.058230

369   Junqueira LC, Assis Figueiredo MT, Torloni H, Montes GS (1986) Differential histologic diagnosis of

370   osteoid. A study on human osteosarcoma collagen by the histochemical picrosirius-polarization

371   method. J Pathol 148:189–196. doi:10.1002/path.1711480210

372   Junqueira LC, Bignolas G, Brentani RR (1979) Picrosirius staining plus polarization microscopy, a

373   specific method for collagen detection in tissue sections. Histochem J 11:447–455. doi:

374   10.1007/BF01002772

375   Kliment CR, Englert JM, Crum LP, Oury TD (2011) A novel method for accurate collagen and

376   biochemical assessment of pulmonary tissue utilizing one animal. Int J Clin Exp Pathol 4:349–355

377   Kulak CA, Dempster DW (2010) Bone histomorphometry: a concise review for endocrinologists and

378   clinicians. Arq Bras Endocrinol Metab 54:87–98. doi: 10.1590/s0004-27302010000200002

379   Moreira CA, Dempster DW, Baron R (2019) Anatomy and ultrastructure of bone – histogenesis, growth

380   and remodeling mdtext.com. https://www.ncbi.nlm.nih.gov/books/NBK279149/. In: Endotext

381   [Internet]. South Dartmouth (MA)

382   Nakata H, Kuroda S, Tachikawa N et al. (2016) Histological and micro-computed tomographic

383   observations after maxillary sinus augmentation with porous hydroxyapatite alloplasts: a clinical case

384   series. Springerplus 5:260. doi: 10.1186/s40064-016-1885-2

385   Niewiesk S, Prince G (2002) Diversifying animal models: the use of hispid cotton rats (*Sigmodon

386   hispidus*) in infectious diseases. Lab Anim 36:357–372. doi: 10.1258/0023677023203889026

387   Noda K, Nakamura Y, Oikawa T et al. (2007) A new idea and method of tooth movement using a ratchet

388   bracket. Eur J Orthod 29:225–231. doi:10.1093/ejo/cjm002

389   Ralis ZA, Watkins G (1992) Modified tetrachrome method for osteoid and defectively mineralized bone

390   in paraffin sections. Biotech Histochem 67:339–345. doi:10.3109/10520299209110046

391   Rentsch C, Schneiders W, Manthey S et al. (2014) Comprehensive histological evaluation of bone

392   implants. Biomatter 4:e27993. doi:10.4161/biom.27993

393   Roach HI, Mehta G, Oreffo RO et al. (2003) Temporal analysis of rat growth plates: cessation of growth

394   with age despite presence of a physis. J Histochem Cytochem 51:373–383. doi:

395   10.1177/002215540305100312

396   Rosset EM, Bradshaw AD (2016) SPARC/osteonectin in mineralized tissue. Matrix Biol 52–54:78–87.

397   doi: 10.1016/j.matbio.2016.02.001

398   Segnani C, Ippolito C, Antonioli L et al. (2015) Histochemical detection of collagen fibers by Sirius

399   red/fast green is more sensitive than van Gieson or Sirius red alone in normal and inflamed rat colon.

400   PLOS ONE 10:e0144630. doi: 10.1371/journal.pone.0144630

401   Tomida S, Aizawa K, Nishida N et al. (2019) Indomethacin reduces rates of aortic dissection and rupture

402   of the abdominal aorta by inhibiting monocyte/macrophage accumulation in a murine model. Sci Rep

403   9:10751. doi: 10.1038/s41598-019-46673-z

404   Ueno T (1985) Comparative study of various methods for identification of osteoid matrix in decalcified

405   bone. Jpn J Oral Biol 27:495–508. doi.org/10.2330/joralbiosci1965.27.495

406   Yoshiki S (1973) A simple histological method for identification of osteoid matrix in decalcified bone.

407   Stain Technol 48:233–238. doi:10.3109/10520297309116630

408

409

Figure legends

Fig. 1 Picrosirius red staining for osteoid detection under both polarized microscopy and light microscopy

(a-d) Representative image of the (a and a') rat femurs, (b and b') caudal vertebrae of cotton rats, (c and c') rabbit femurs, and (d and d') rat femurs decalcified by indicated conditions. The sections were stained with 1% picrosirius red for 1 h. (e and e') Optimal conditions for osteoid staining by picrosirius red under light microscopy. The rat femurs with over-decalcification were stained with 1% alcian blue (pH 2.5) followed by picrosirius red of indicated conditions. Arrowheads: osteoid, arrows: mineralized bone, HZ: hypertrophic zone, PZ: proliferating zone.

Fig. 2 Comparison of the dyes for staining of the mineralized bone combined with picrosirius red

Representative image of the mineralized bone. The rabbit femurs decalcified with inorganic acid were stained with Weigert's iron hematoxylin, 0.75% orange G, followed by staining with (a-a'') aniline blue, (b-b'') fast green FCF, (c-c'') light green SF, and (d-d'') naphthol green B of the indicated concentrations, and finally with 0.04% picrosirius red. The sections were treated with 2.5% phosphomolybdic acid and 2.5% phosphotungstic acid as a mordant. Asterisks indicate the faint staining area of the mineralized bone. LB: lamellar bone.

Fig. 3 Identifying a suitable specimen thickness and mordant for JFRL staining

(a-a''') Specimen thickness suitable for the distinguishment of osteoid and mineralized bone. Serially sliced sections of rabbit femurs decalcified with inorganic agents are shown. (b and b') Comparison of the mordants for JFRL staining. Sections of mice femurs decalcified with a chelator were treated with 2.5% phosphotungstic acid and 2.5% phosphomolybdic acid (upper panel) and saturated picric acid (lower

433   panel) as a mordant. (c-d') Comparison of bone staining between JFRL staining and picrosirius red

434   staining under light microscopy and polarized microscopy, respectively. Sections of rabbit femurs

435   decalcified with organic acid and sections of over-decalcified rat femurs are shown. Arrows: the color

436   overlap in mineralization front, arrowheads: osteoid, asterisks: osteocytes, Ca: cartilage, E: erythrocytes,
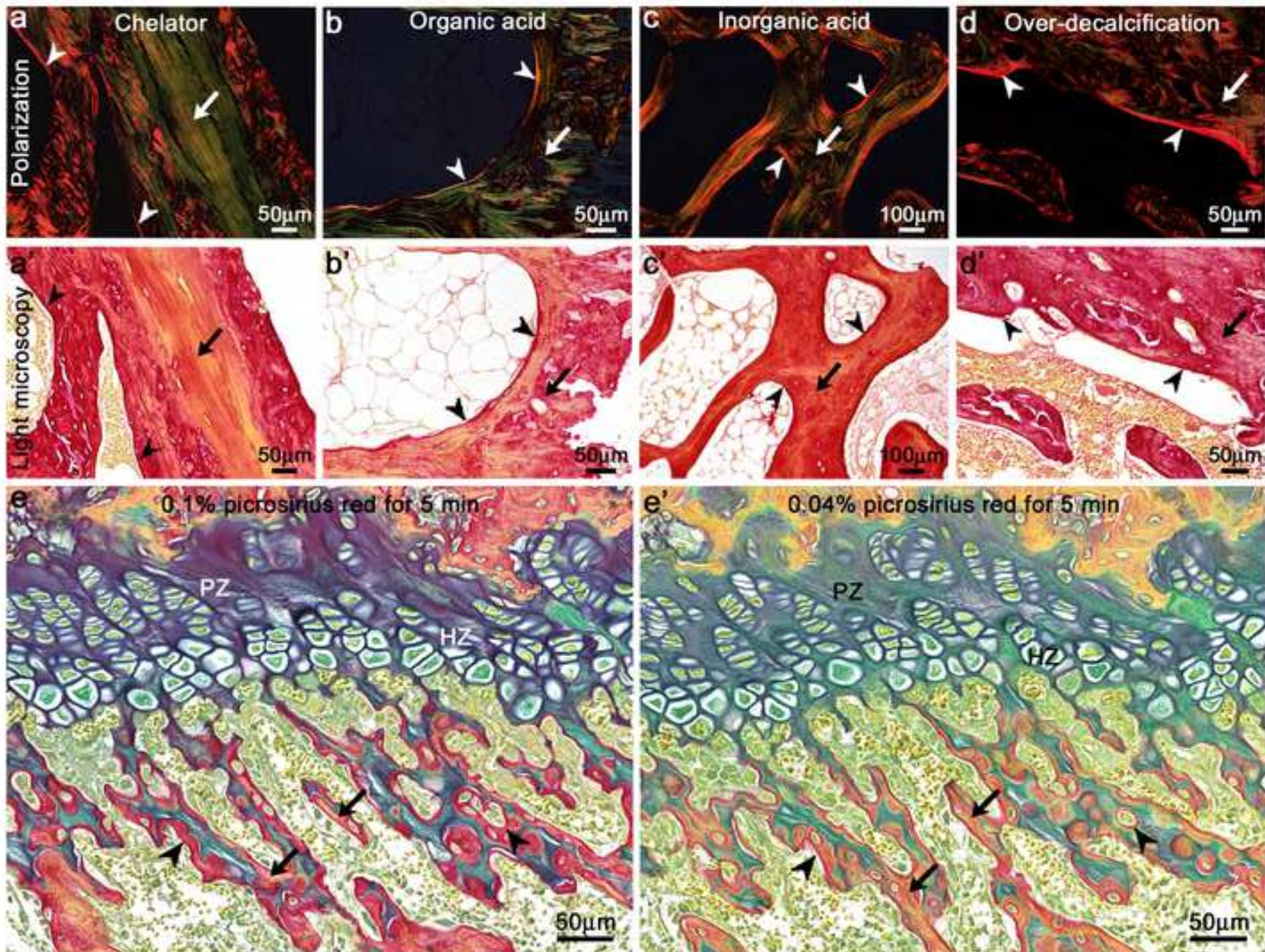
437   LB: lamellar bone, WB: woven bone.

438

439   **Fig. 4 Simultaneous detection of osteochondral matrix and bone cells in endochondral ossification**
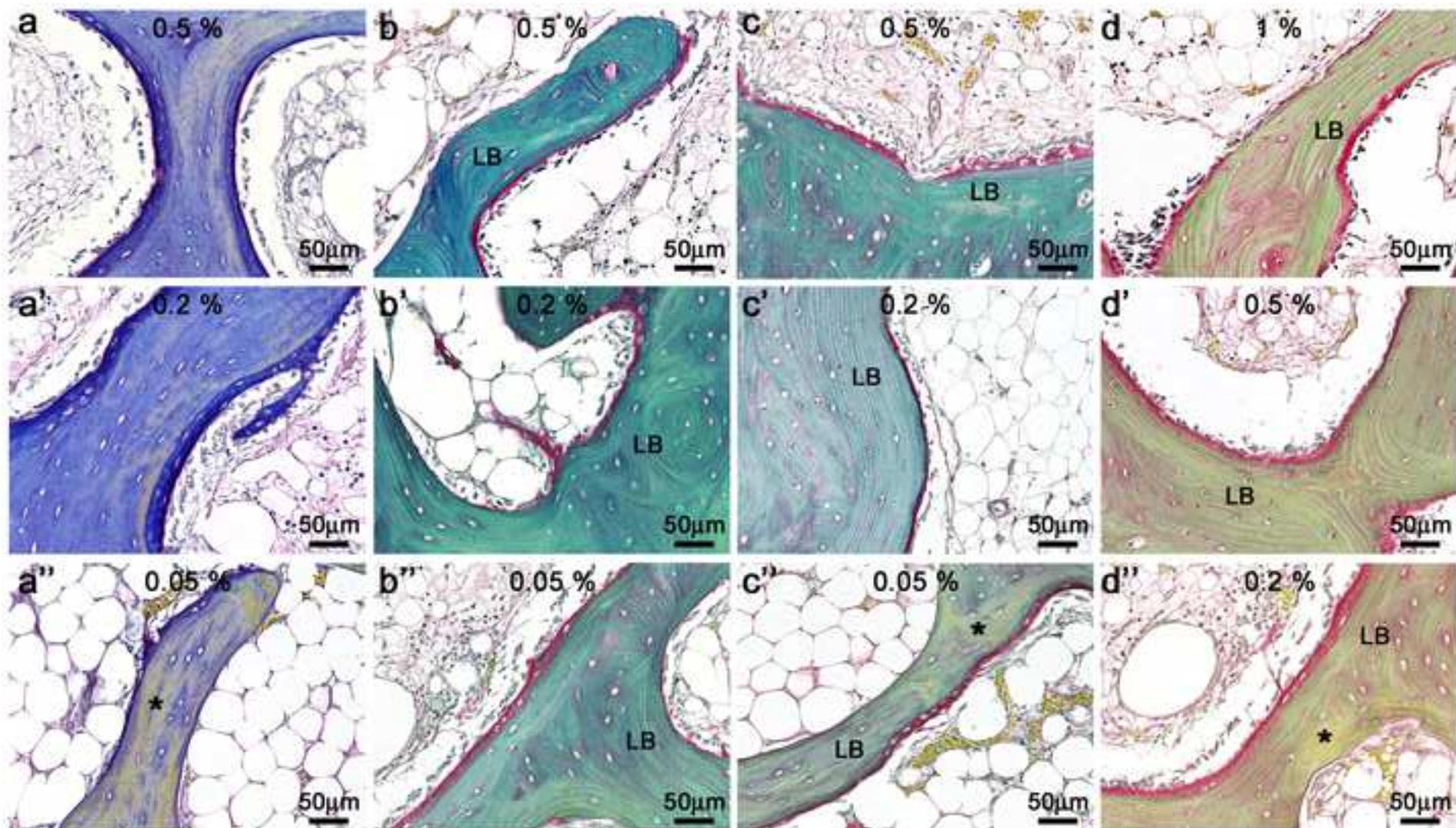
440   Endochondral ossification of the rat femur (a-c) decalcified with organic acid or (a'-c') those with over-

441   decalcification. Representative images of JFRL staining using (a and a') 0.05% picro-fast green FCF, (b

442   and b') 0.5% picro-light green SF, or (c and c') 1% picro-naphthol green B are shown. The black box is

443   magnified in the lower-left panel. Ca: cartilage of the trabeculae, HZ: hypertrophic zone, MB: mineralized

444   bone, Ob: osteoblasts, Oc: osteoclasts, Os: osteoid, PZ: proliferating zone.
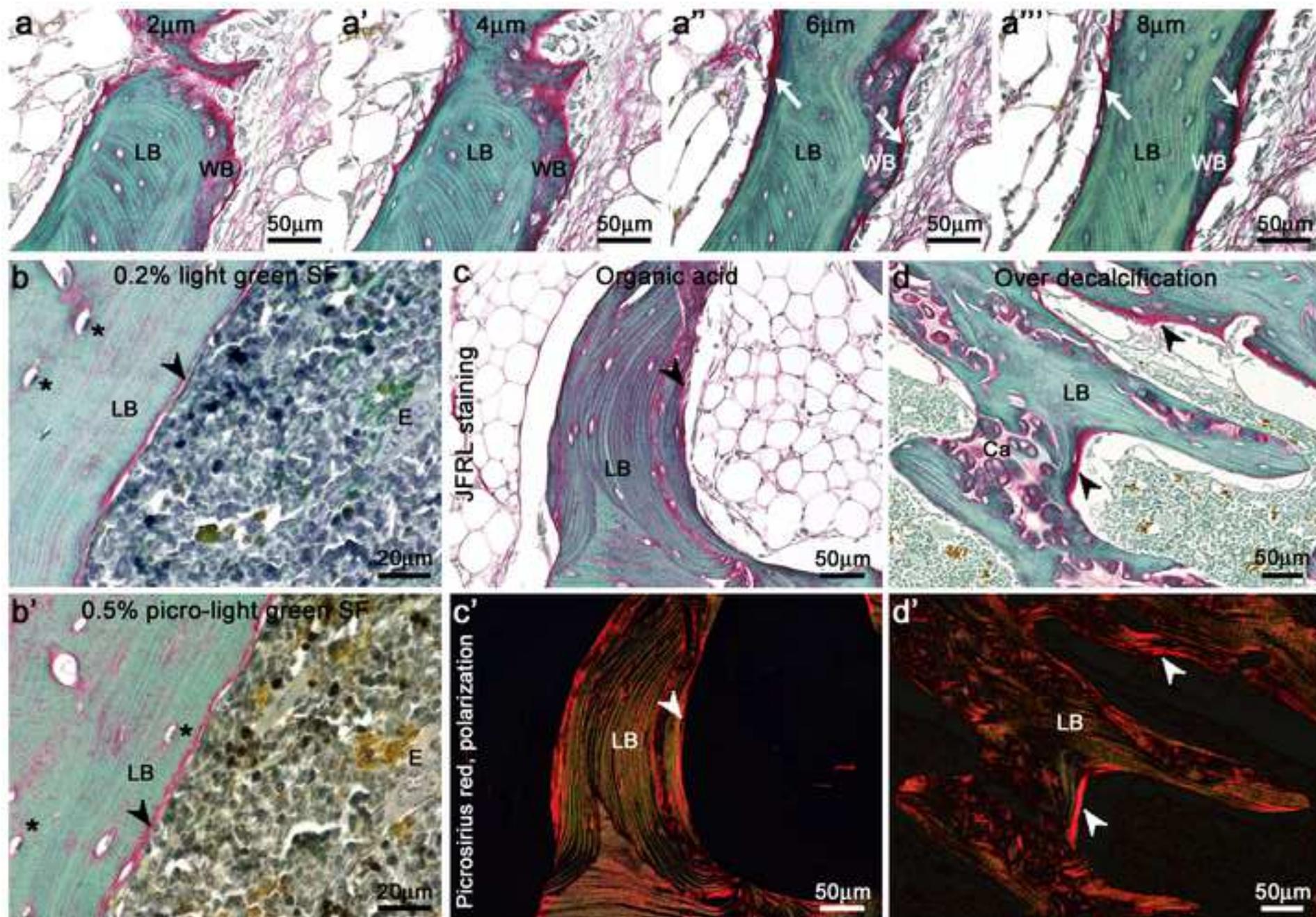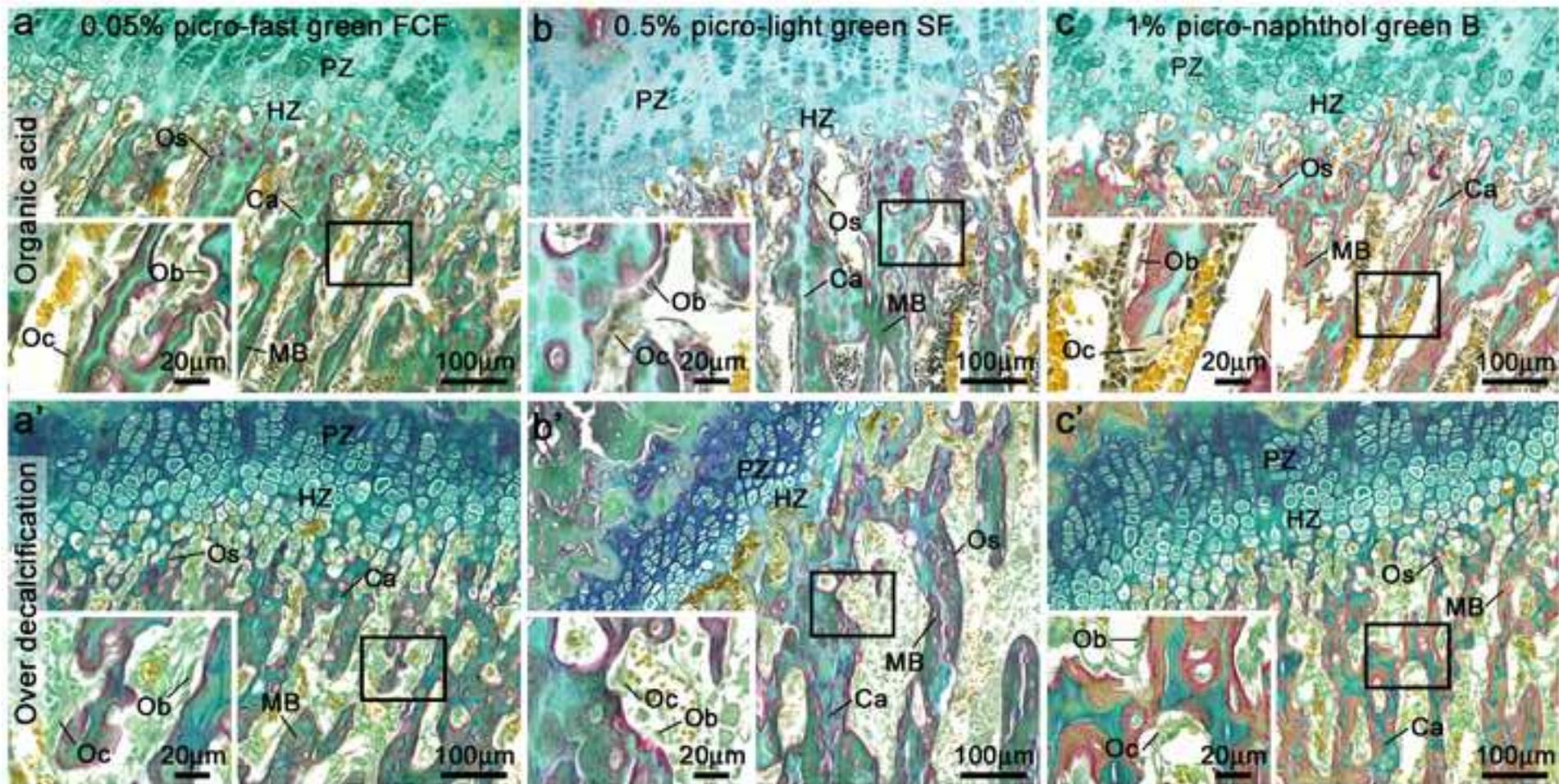
445

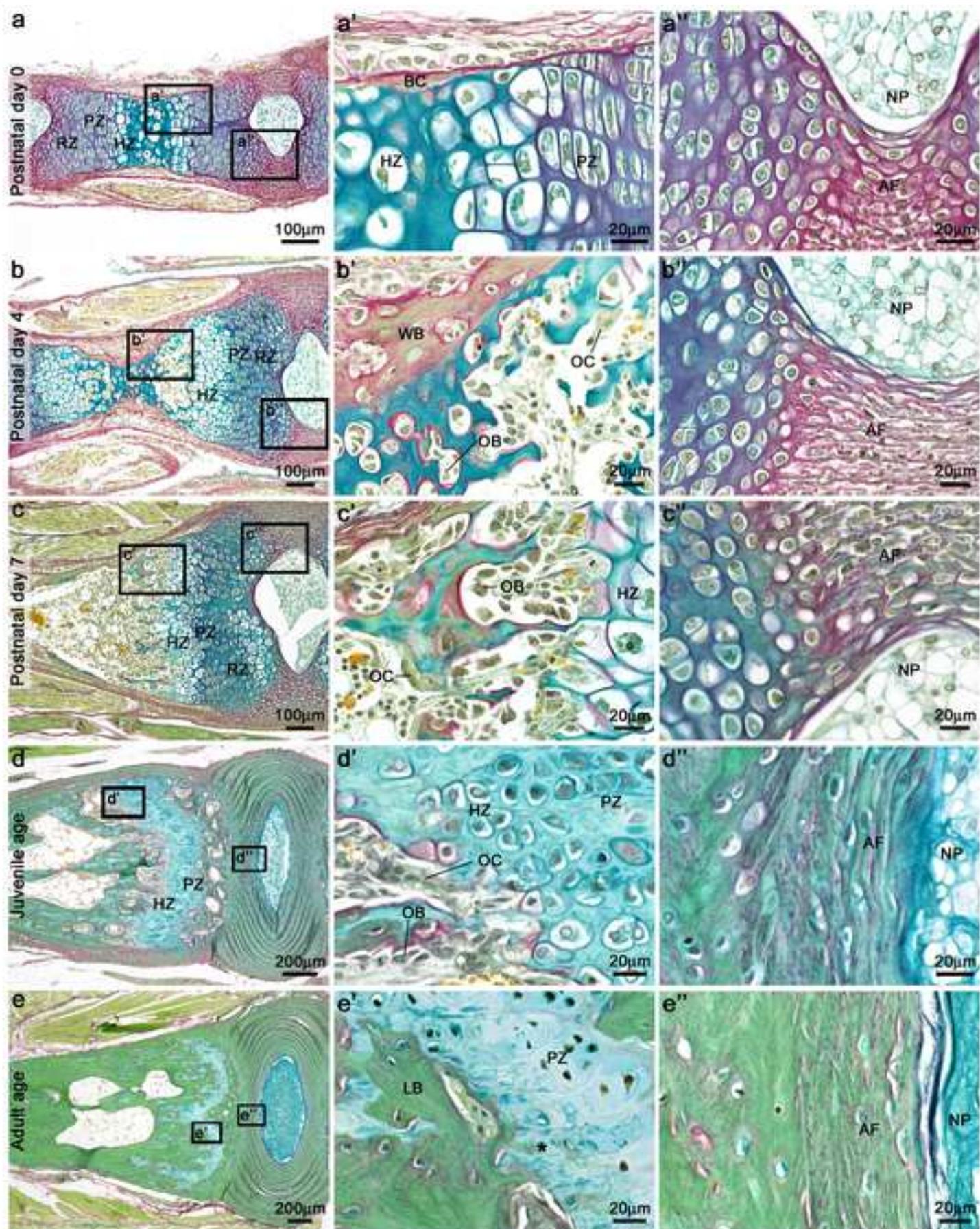446   **Fig. 5 Age-related changes in the caudal vertebrae of cotton rats**

447   (a-e) Longitudal sections of the caudal vertebrae of cotton rats decalcified with organic acid. Black boxes

448   are magnified in the next panel showing the (a'-e') hyaline cartilage and (a''-e'') fibrocartilage. Asterisk

449   indicates bone formation within the epiphyseal plate. AF: annulus fibrosus, BC: bone collar, HZ:

450   hypertrophic zone, LB: lamellar bone, NP: nucleus pulposus, Ob: osteoblasts, Oc: osteoclasts, Os: osteoid,

451   PZ: proliferating zone, RZ: resting zone, WB: woven bone.

Figure 1

Figure 2

Figure 3

Click here to access/download;Figure;Figure3.tif

Figure 4

Click here to access/download;Figure;Figure4.tif ⬇

1 **Table 1. List of animal species and decalcification methods for bone specimens**

Principle	Chelator	Organic acid	Inorganic acid	Over-decalcification
Decalcification				
Solution	10% EDTA2Na	Morse's solution	K-CX solution	K-CX solution
pH	7.0	2.5	0.2	0.2
Condition	2 to 12 weeks	5 to 14 days	1 to 3 days	4 to 5 days
	at RT	at RT	at 4 °C	at RT
Animals, bones				
Mice, femurs	5	6	ne	ne
Cotton rats, caudal vertebrae	6	19	ne	ne
Rats, femurs	5	8	8	6
Rabbits, femurs and tibiae	7	10	10	6

2 RT: room temperature, ne: not examined. For the cotton rats, caudal vertebrae on 0 day (n=3), 4 days

3 (n=3), 7 days (n=4), 2 months (n=3), and 6 months (n=6) of age were fixed with 10 % neutral buffered

4 formalin and decalcified with Morse's solution.

1 **Table 2 Summary of staining characteristics by JFRL staining**

Structure	Color	Corresponding dyes
Cartilage matrix		
Hyaline cartilage	Blue to purple	Alcian blue
Fibrocartilage	Blue, green, and red	Alcian blue, light green SF, sirius red
Bone matrix		
Osteoid	Red	Sirius red
Mineralized bone	Green	Light green SF
Lamellar bone	Green with repeated sequences of red line	Light green SF, sirius red
Woven bone	Green with various degrees of red patches	Light green SF, sirius red
Cells		
Osteoblasts	Single nucleus with blackish cytoplasm	Weigert's iron hematoxylin
Osteocytes	Single nucleus with oval shape	Weigert's iron hematoxylin
Osteoclasts	Multiple nuclei with greenish cytoplasm	Weigert's iron hematoxylin, light green SF
Erythrocytes	Yellow to orange	Orange G
Cell nuclei	Black to dark brown	Weigert's iron hematoxylin
Cytoplasm	Various colors	Weigert's iron hematoxylin, light green SF

2 The color of the cartilage matrix depends on the age and decalcification conditions. The green of the mineralized bone varies from

3 yellowish green to bluish green depending on the dye and solvent used.

Electronic supplementary material

Title:

Novel Polychrome Staining Distinguishing Osteochondral Tissue and Bone Cells in Decalcified Paraffin Sections

Journal name:

Cell and Tissue Research

Authors:

Teppei Nakamura, Kanako Sumi, Erika Tsuji, Marina Hosotani, Takashi Namba, Osamu Ichii, Takao Irie, Ken-ichi Nagasaki, Yasuhiro Kon, Takashi Mishima, Tomoji Yoshiyasu

Corresponding author:

Teppei Nakamura, D.V.M., Ph.D

Department of Biological Safety Research, Chitose Laboratory, Japan Food Research Laboratories, Chitose, Hokkaido 066-0052, Japan

E-mail: nakamurate@jfrl.or.jp

Supplemental Table 1. Procedure of Join of the Five dyes Revealing coLlagenous tissue (JFRL) staining

Process	Method	Critical step and troubleshooting
Fixation	☐ Fix with 10 % neutral buffered formalin at RT.	
Decalcification	☐ Routinely decalcify with chelators (e.g., EDTA), organic acids (e.g., formic acid), or inorganic acids (e.g., hydrochloric acid) [1].	✓ Over-decalcification is also applicable, but the nuclear staining becomes faint in this condition.
Tissue processing	☐ Routinely perform and embed the specimen in paraffin.	
Slice	☐ Prepare bone sections at 4-μm thickness.	✓ Thinner sections tend to increase red intensity. ✓ Thicker sections tend to increase green intensity.
Deparaffinization	☐ Routinely perform.	
Cartilage staining (if necessary)	☐ Immerse in 3 % acetic acid. ☐ Stain with 1 % alcian blue solution (pH2.5) for 20 min at RT. ☐ Wash with 3 % acetic acid.	
Nucleus staining	☐ Stain with Weigert's iron hematoxylin for 10 min at RT. ☐ Wash with tap water.	✓ Differentiation can be omitted.
Red blood cell staining	☐ Stain with 0.75% orange G for 2 min at RT. ☐ Wash with 1% acetic acid.	✓ Avoid washing with tap water as this may cause orange G to fade.
Mineralized bone staining	☐ Stain with 0.5% picro-light green SF for 3 min at RT. ☐ Wash with 1% acetic acid.	✓ 1% picro-naphthol green B are applicable instead of picro-light green SF.
Osteoid staining	☐ Stain with 0.04% picrosirius red solution for 5–10 min at RT. ☐ Wash with 1% acetic acid.	✓ Shorten this process in case of intense red color. ✓ Lengthen this process in case of intense green color.
Dehydration and coverslip	☐ Routinely perform and coverslip using a non-aqueous mounting media.	✓ Immerse sections in alcohol and xylene until the removal of excess picric acid.

RT: room temperature, EDTA: ethylenediaminetetraacetice acid. Solution of 0.75% orange G: dissolve orange G in distilled water. Solution of 0.5% picro-light green SF and 1% picro-naphthol green B: dilute 2% solution of each dye with saturated picric acid. Solution of 0.04% picrosirius red: dilute 1% sirius red solution with saturated picric acid.

[1] Shibata Y, Fujita S, Takahashi H et al. (2000) Assessment of decalcifying protocols for detection of specific RNA by non-radioactive in situ hybridization in calcified tissues. Histochem Cell Biol 113:153–159. doi: 10.1007/s004180050434